The Suggested Electrode Number in Electrocardiographic Imaging for Identifying Atrial Fibrillation Drivers

Zhang Yadan[1,2], Wu Jian[2], Xiang Min[1], Cui Yangyang[1]

[1]Hangzhou Institute of National Extremely-weak Magnetic Field Infrastructure, Hangzhou , China
[2]Institute of Biomedical Engineering, Shenzhen International Graduate School, Tsinghua University, Shenzhen, China

Abstract

Electrocardiographic imaging (ECGI) is expected to map the epicardial potential non-invasively and globally and identify the atrial fibrillation (AF) drivers, which may compensate for the imprecision and incompleteness of the current intracardiac catheter mapping for AF drivers. There is currently no uniform standard in ECGI for the selection of the ideal electrode number on the body surface. To determine the optimal number of body surface electrodes for identifying the AF driving source, we conducted a comparison of the relevance and accuracy of the reconstructed epicardial potentials in ECGI when the electrode configurations tested were 128, 112, 96, 80, 72, 64, 48, 32, 24, and 12. After reviewing and analyzing the results acquired from 10 individuals with paroxysmal or persistent AF, we discovered that for persistent AF, the recommended number of electrodes is 64 or more, whereas for paroxysmal AF, the minimum number of electrodes is 48. This finding can be used as a foundation for selecting the number of body surface electrodes in ECGI, hence enhancing the clinical application efficiency and usefulness of ECGI in identifying the driving source of AF.

1. Introduction

Electrocardiographic imaging (ECGI), a noninvasive approach for mapping epicardial electrical activity, is expected to non-invasively identify the atrial fibrillation (AF) driver sources [1]. The mathematical expression for the ECGI inverse problem is $\Phi_H = A^{-1} \cdot \Phi_B$, where Φ_B is the high-density body surface potential signals (BSPs, i.e., ECG signals on the body surface) and A is the transfer matrix, Φ_H is the epicardial electrical activity to be solved [2]. The number of high-density body surface electrodes is one of the most influential aspects in the accuracy of solution to the ECGI inverse problem [3]. Despite the fact that numerous studies have investigated the ideal number and distribution of electrodes on the body surface for ECGI, there is currently no uniform standard for the optimal number and placement of electrodes for ECGI. Typically, 12 to 300 electrodes are used in ECGI [4-6]. The installation of high-density electrodes and their fixation on the surface of the torso are time-consuming, and a great deal of redundant information will be acquired if the number of electrodes is too large, which cannot aid in the identification of the source of AF [7]. To improve the measuring efficiency of high-density BSPs, this study is to explore the recommended number of body surface electrodes that is most conducive to the identification of the AF driving source.

2. Methods

The whole research procedure is depicted in Figure 1. An enhanced spectral clustering technique was developed to unsupervised screening the varying numbers of electrodes from 128 electrodes.

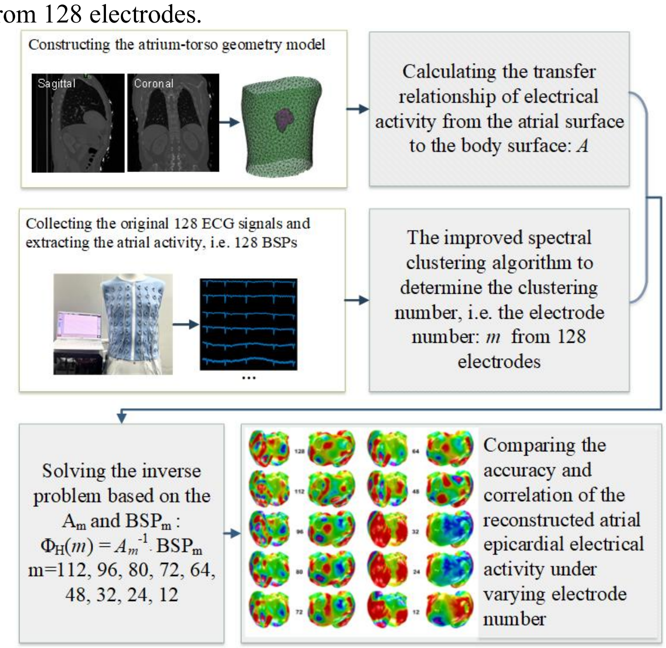

Figure 1. The overall research process.

Compared to standard spectral clustering, this work enhances the creation approach of the similarity. We use

 ISSN: 2325-887X DOI: 10.22489/CinC.2024.002

cosine distance and standardized Euclidean distance to measure the similarity between different objects. The following are the improved spectral clustering algorithm steps [8]:

i. Construct the similarity matrix W between points, $W = (1-\alpha) \cdot W_C + \alpha \cdot W_E$, where W_C is the cosine distance and W_E represents the standardized Euclidean distance. α is the weight coefficient to balance the W_C and W_E.

ii. Determine the degree matrix D based on the similarity matrix, $D = \mathrm{diag}(d_1, d_2, \ldots, d_n)$, $d_i = \sum_{j=1}^{n} w(i,j)$.

iii. Calculate the Laplacian matrix L, $L = D - W$.

iv. Perform dimensionality reduction on the matrix L.

v. Perform K-means clustering to get the final clustering result.

Considering that the conduction of cardiac electrical activity has both direction and size, which can respectively reflect the direction and size characteristics of atrial activity [9]. We employed a weighted average of the cosine distance and the standardized Euclidean distance to ensure that the two distances are of the same order of magnitude and have the same level of influence on the evaluation of similarity results.

This study employed the boundary element algorithm [10] to solve the transfer matrix A and our previously reported time-frequency domain inverse problem-solving scheme [11, 12] to solve the atrial surface electrical activity Φ_H based on the varied electrode numbers. To extract atrial activity from high-density surface ECG signals, QRS waves and T waves were first excluded from this investigation. Analyzing the accuracy and correlation of the reconstructed atrial electrical activity under varying numbers of electrodes determines the suggested minimum electrode number sufficient for the localization of the AF driving source.

3. Results

3.1. Experimental Datasets

10 AF cases were included in this study, including 6 paroxysmal AF and 4 persistent AF patients. The surgeon performed invasive electrophysiological mapping (Biosense Webster) with the help of the Carto 3 system, performed pulmonary vein isolation and linear ablation on these patients.

In this study, the ActiveTwo system (Biosemi BV, Amsterdam, The Netherlands) was used to collect high-density BSPs of these patients, and the sampling frequency was 2048Hz; The enhanced left atrium(LA)-pulmonary vein(PV) computed tomography (CT) images of AF patients were collected, and the three-dimensional segmentation and reconstruction of LA, right atrium(RA), torso and electrodes were completed with the help of MIMICS software.

This study was approved by the local ethics committee, and all patients completed consent forms.

3.2. Experimental design

From the original 128 surface electrodes, we selected out 112, 96, 80, 72, 64, 48, 32, 24, and 12 electrodes using the enhanced spectral clustering approach. By examining the relevance and correctness of atrial epicardial electrical activity reconstructed by the ECGI under varying numbers of body surface electrodes, the suggested minimum numbers of electrodes for paroxysmal and persistent AF are identified, respectively.

3.3. Experimental Results

Figure 2 (a) depicts the reconstructed atrial epicardial potential map of a patient with paroxysmal AF using a variety of electrode configurations. The red area depicts the area of low voltage calculated by ECGI, which is predominantly dispersed around PV. As the number of electrodes diminishes, so does the resolution of the reconstructed potential map. When the number of electrodes was lowered to 32 or less, the reconstructed low voltage area around the PV began to diverge dramatically from the catheter mapping low voltage area.

During the operation, the catheter assessed the potential distribution on the atrium as depicted in Figure 2 (b). The white ellipse indicates the region of low voltage measured by the catheter, which is mostly dispersed in the left and right PV as well as the posterior wall of the LA. In Figure 2 (a), there is a high degree of resemblance between the reconstructed low-voltage zone for 48 or more electrodes and the low-voltage region mapped by the catheter in Figure 2(b), demonstrating that the reconstructed epicardial potential in this study is therapeutically effective.

Figure 2 (c) depicts the correlation coefficient (CC) between the atrial potential maps reconstructed using ECGI with varying numbers of electrodes selected using the enhanced spectral clustering algorithm. For 48 electrodes and above, the CC between the potential maps reconstructed by ECGI is between 0.85 and 0.99; when the number of electrodes is less than 48, the CC between the reconstructed potential maps drops sharply below 0.33, indicating that when the number of electrodes is less than 48, the reconstructed atrial potential maps are quite different from those of a higher number of electrodes.

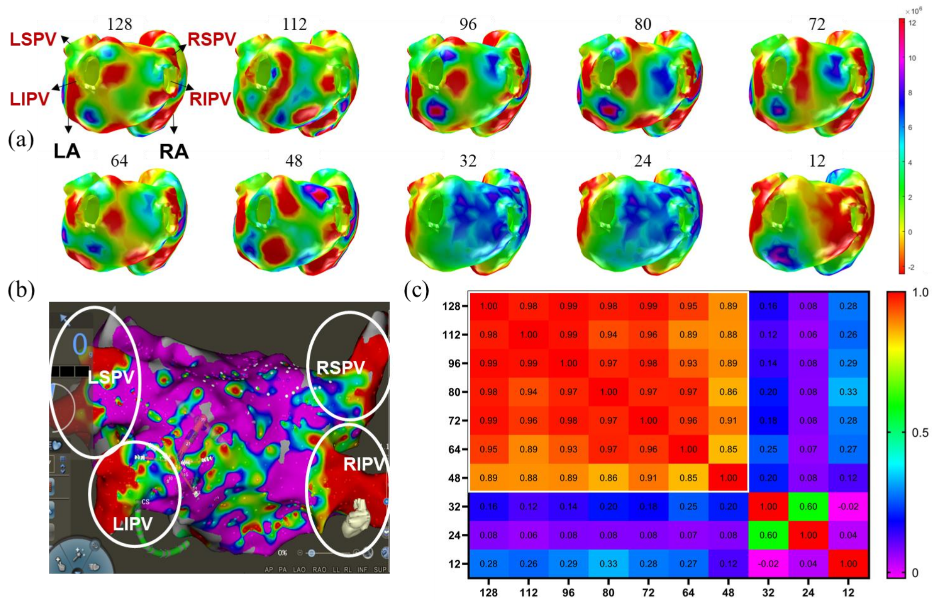

Figure 2. An instance of paroxysmal AF: (a) Atrial surface potential map reconstructed by ECGI under different numbers of electrodes, red represents low voltage area;(b) The voltage map of the intracardiac catheter mapping, the red area circled by the white oval in the figure is the low voltage area mapped by the intracardiac catheter;(c) CC between atrial surface potentials reconstructed by ECGI under different electrodes. LIPV, left inferior pulmonary vein; LSPV, left superior pulmonary vein; RIPV, right inferior pulmonary vein; RSPV, right superior pulmonary.

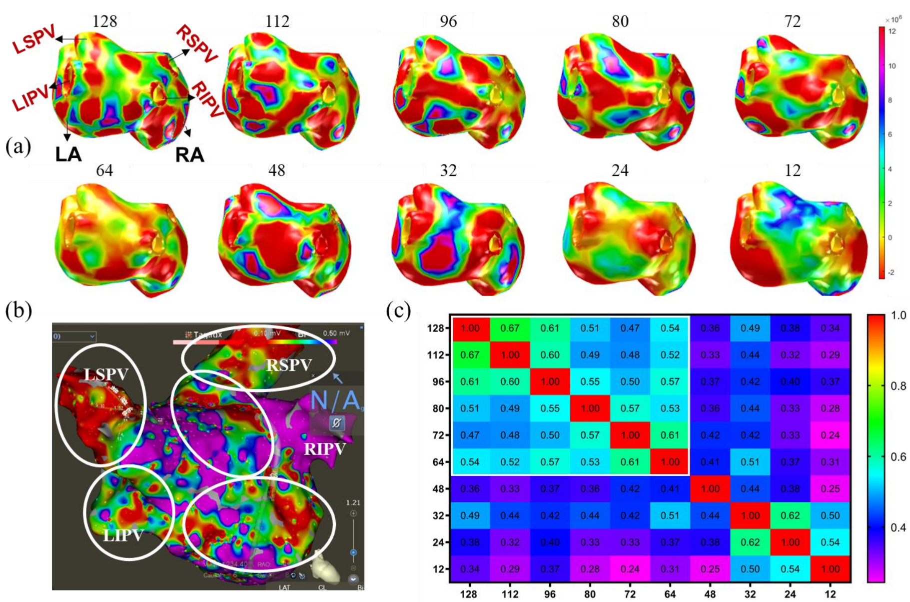

Figure 3. An example of persistent AF: (a) Atrial surface potential maps reconstructed by ECGI under different numbers of electrodes, red represents low voltage area;(b) The voltage map of the intracardiac catheter mapping, the red area circled by the white oval in the figure is the low voltage area mapped by the intracardiac catheter;(c) CC between atrial surface potentials reconstructed by ECGI under different electrodes.

Figure 3 depicts an example of persistent AF case. Similar to Figure 2, Figure 3(a) depicts the atrial epicardial potential maps reconstructed by ECGI in varying electrode numbers. Figure 3(b) shows the potential distribution mapped by the intracardiac catheter , and Figure 3(c) depicts the CC between the potential maps reconstructed by ECGI under different numbers of electrodes. The intracardiac catheter discovered low-voltage regions primarily around the left and right PV and the back and bottom of the atrium. In Figure 3(a), although the resolution of the potential map reconstructed by ECGI is lower than that of the catheter mapping voltage map, the reconstructed potential maps with 64 or more electrodes demonstrate that the abnormal electrical activity areas of the LA are also distributed around the left and right pulmonary veins as well as the back and bottom of the atrium. In Figure 3(c), the correlation between the potential maps with 64 or more electrodes is strong, and the CC is greater than 0.47; as the number of electrodes decreases, the reconstructed potential maps are significantly different from the reconstruction results obtained with a larger number of electrodes, and the CC also are significantly lower as a whole.

4. Discussion

Through the study of data from 6 cases of paroxysmal AF and 4 cases of persistent AF, we discovered that when the number of body surface electrodes reduces, the resolution of the atrial potential map rebuilt by ECGI also decreases, which is consistent with the literature [3]. For paroxysmal AF, the minimum number of electrodes required to achieve a potential map reconstruction comparable to that of a higher number of electrodes is 48; for persistent AF, the minimum number of electrodes must be greater than 48 (such as 64 or above) to achieve an effective potential map reconstruction. As the maintenance mechanism of persistent AF is more complex than that of paroxysmal AF, it is fair to require a greater number of surface electrodes in ECGI for persistent AF than for paroxysmal AF.

5. Conclusion

With the aid of an unsupervised spectral clustering technique, the minimal number of electrodes most suitable for identifying AF driver sources in ECGI is investigated in this work. For persistent AF, it is recommended that the minimum number of electrodes be greater than 48 (such as 64 and above); for paroxysmal AF, when the minimum number of electrodes is 48, the reconstructed potential map can maintain a high similarity with the reconstruction results obtained by ECGI with higher number of electrodes.

Acknowledgments

Research supported by the Knowledge Innovation Program of Basic Research Projects of Shenzhen [JCY20200109142805928， JCYJ20160428182053361], in part by National Key R&D Program of China (2019YFC0119500).

References

[1] Salinet, João, Rubén Molero, Fernando Schlindwein, et al. "Electrocardiographic Imaging for Atrial Fibrillation: A Perspective from Computer Models and Animal Experiments to Clinical Value." Frontiers in Physiology 12 (2021): 653013.

[2] Cluitmans, Matthijs, Dana H Brooks, Rob MacLeod, et al. "Validation and Opportunities of Electrocardiographic Imaging: From Technical Achievements to Clinical Applications." Frontiers in Physiology 9 (2018): 1305.

[3] Marques, Victor Gonçalves, Miguel Rodrigo, et al. "Characterization of Atrial Arrhythmias in Body Surface Potential Mapping: A Computational Study." Computers in Biology and Medicine 127 (2020): 103904.

[4] Xujian Feng, Baodan Bai, Ziqian Wu, et al. "Leads Selection of Body Surface Potential Mapping During Atrial Fibrillation: A Sequential Selection Based on Adapted Botteron's Approach." IEEE Access 7 (2019): 158064-58074.

[5] Rodrigo, M., A.M. Climent, A. Liberos, et al. "Minimal Configuration of Body Surface Potential Mapping for Discrimination of Left versus Right Dominant Frequencies during Atrial Fibrillation." Pacing and Clinical Electrophysiology 40, no. 8 (2017): 940-46.

[6] Parreira, L. , et al. "Electrocardiographic imaging (ECGI): What is the minimal number of leads needed to obtain a good spatial resolution?." Journal of Electrocardiology 62(2020).

[7] Finlay, Dewar D, Chris D Nugent, Mark P Donnelly, Robert L Lux, Paul J McCullagh, and Norman D Black. "Selection of Optimal Recording Sites for Limited Lead Body Surface Potential Mapping: A Sequential Selection Based Approach." BMC Medical Informatics and Decision Making 6, no. 1 (2006): 9.

[8] Wen, G. (2020) "Robust self-tuning spectral clustering," Neurocomputing (Amsterdam), 391, pp. 243–248.

[9] He, Hong, Yonghong Tan, and Jianfeng Xing. "Unsupervised Classification of 12-lead ECG Signals Using Wavelet Tensor Decomposition and Two-dimensional Gaussian Spectral Clustering." Knowledge-based Systems 163 (2019): 392-403.

[10] Wrobel, Luiz C. Boundary Element Method Part 1 Heat Transfer. Emerald Group Publishing Limited, 2003.

[11] Yadan, Zhang, Lian Xin, and Wu Jian. "Solving the Inverse Problem in Electrocardiography Imaging for Atrial Fibrillation Using Various Time-frequency Decomposition Techniques Based on Empirical Mode Decomposition: A Comparative Study." Frontiers in Physiology 13 (2022): 999900.

[12] Yadan Z, Jian W, Yifu L, et al. "Solving the inverse problem based on UPEMD for electrocardiographic imaging." Biomedical Signal Processing and Control 76(2022): 103665.

Address for correspondence:

Wu Jian
Institute of Biomedical Engineering, Shenzhen International Graduate School, Tsinghua University, Shenzhen, China
wuj@sz.tsinghua.edu.cn

Xiang Min and Cui Yangyang
Hangzhou Institute of National Extremely-weak Magnetic Field Infrastructure, Hangzhou 310028, China
xiangmin@buaa.edu.cn, cuiyy20@mails.tsinghua.edu.cn